AMERICAN SOCIETY FOR MICROBIOLOGY | Journal of Virology

Cell-to-Cell Contact and Nectin-4 Govern Spread of Measles Virus from Primary Human Myeloid Cells to Primary Human Airway Epithelial Cells

Brajesh K. Singh,[a] Ni Li,[a] Anna C. Mark,[a] Mathieu Mateo,[b]* Roberto Cattaneo,[b] Patrick L. Sinn[a]

Stead Family Department of Pediatrics, Carver College of Medicine, The University of Iowa, Iowa City, Iowa, USA[a]; Department of Molecular Medicine, Mayo Clinic, Rochester, Minnesota, USA[b]

ABSTRACT

Measles is a highly contagious, acute viral illness. Immune cells within the airways are likely first targets of infection, and these cells traffic measles virus (MeV) to lymph nodes for amplification and subsequent systemic dissemination. Infected immune cells are thought to return MeV to the airways; however, the mechanisms responsible for virus transfer to pulmonary epithelial cells are poorly understood. To investigate this process, we collected blood from human donors and generated primary myeloid cells, specifically, monocyte-derived macrophages (MDMs) and dendritic cells (DCs). MDMs and DCs were infected with MeV and then applied to primary cultures of well-differentiated airway epithelial cells from human donors (HAE). Consistent with previous results obtained with free virus, infected MDMs or DCs were incapable of transferring MeV to HAE when applied to the apical surface. Likewise, infected MDMs or DCs applied to the basolateral surface of HAE grown on small-pore (0.4-μm) support membranes did not transfer virus. In contrast, infected MDMs and DCs applied to the basolateral surface of HAE grown on large-pore (3.0-μm) membranes successfully transferred MeV. Confocal microscopy demonstrated that MDMs and DCs are capable of penetrating large-pore membranes but not small-pore membranes. Further, by using a nectin-4 blocking antibody or recombinant MeV unable to enter cells through nectin-4, we demonstrated formally that transfer from immune cells to HAE occurs in a nectin-4-dependent manner. Thus, both infected MDMs and DCs rely on cell-to-cell contacts and nectin-4 to efficiently deliver MeV to the basolateral surface of HAE.

IMPORTANCE

Measles virus spreads rapidly and efficiently in human airway epithelial cells. This rapid spread is based on cell-to-cell contact rather than on particle release and reentry. Here we posit that MeV transfer from infected immune cells to epithelial cells also occurs by cell-to-cell contact rather than through cell-free particles. In addition, we sought to determine which immune cells transfer MeV infectivity to the human airway epithelium. Our studies are based on two types of human primary cells: (i) myeloid cells generated from donated blood and (ii) well-differentiated airway epithelial cells derived from donor lungs. We show that different types of myeloid cells, i.e., monocyte-derived macrophages and dendritic cells, transfer infection to airway epithelial cells. Furthermore, cell-to-cell contact is an important component of successful MeV transfer. Our studies elucidate a mechanism by which the most contagious human respiratory virus is delivered to the airway epithelium.

Measles virus (MeV) is extremely contagious and infects its human host via the respiratory route. For many years, MeV was thought to enter through the apical surface of airway epithelial cells (1), a misconception based on studies performed with polarized immortalized cell lines (2, 3). Using well-differentiated primary cultures of airway epithelial cells from human donors (HAE), we demonstrated that MeV has a clear preference for basolateral entry (4). HAE differentiate into a pseudostratified columnar epithelium sheet comprised of ciliated, nonciliated, basal, and goblet cells. This model system is highly representative of the *in vivo* airways (5). MeV infection of HAE results in the formation of infectious centers that, unlike syncytia, retain intact plasma membranes (4, 6, 7). MeV-mediated infectious-center formation in HAE differs from that of most paramyxoviruses (7) and may result from the unique receptor specificity of the *Morbillivirus* genus (8–11). Indeed, we have shown that infectious-center formation in HAE results from direct cell-to-cell spread and is facilitated by the nectin-4/afadin complex (7). These studies highlight the importance of using an appropriate model system to study MeV entry and spread.

How MeV eventually reaches the airway epithelium during a natural infection is less clear. Initially, the infection may be ferried through the epithelium by myeloid cells that sample the airway lumen and express the primary MeV receptor signaling lymphocyte activation molecule family member 1 (SLAMF1, also known

Received 11 February 2016 **Accepted** 11 May 2016

Accepted manuscript posted online 18 May 2016

Citation Singh BK, Li N, Mark AC, Mateo M, Cattaneo R, Sinn PL. 2016. Cell-to-cell contact and nectin-4 govern spread of measles virus from primary human myeloid cells to primary human airway epithelial cells. J Virol 90:6808–6817. doi:10.1128/JVI.00266-16.

Editor: D. S. Lyles, Wake Forest School of Medicine

Address correspondence to Patrick L. Sinn, patrick-sinn@uiowa.edu.

* Present address: Mathieu Mateo, Unité de Biologie des Infections Virales Emergentes, Institut Pasteur, Lyon, France; Centre International de Recherche en Infectiologie (CIRI), Université de Lyon, INSERM U1111, Ecole Normale Supérieure de Lyon, Université Lyon 1, CNRS UMR5308, Lyon, France.

as CD150) (12). In transgenic mice expressing human SLAM, MeV replication was observed in lung resident myeloid cells 24 h after experimental infection (13). Subsequent infection phases were documented for nonhuman primates. MeV replicated vigorously in primary and secondary lymphatic organs of cynomolgus macaques 3 to 5 days after inoculation (14). A few days later, most infected cells in the upper airways were of lymphoid or myeloid origin (15). MeV replication in airway epithelial cells was not observed until the second week following infection (16, 17). Infected myeloid cells were observed below infectious centers in the lamina propria of the trachea. We posited that dendritic cells (DCs) or macrophages must deliver MeV to airway epithelial cells; however, based on available information, the mechanism of this viral transfer remained unknown.

MeV is the most contagious human respiratory virus (18), and within natural hosts, infections appear to remain largely cell associated (19). No free virus is detected in blood of humans or experimentally infected monkeys, for which virus titers are measured by overlaying leukocytes onto SLAM-expressing cells. Only small amounts of cell-free virus can be isolated from respiratory tract secretions (19). In cultured cells, MeV particles accumulate below the plasma membrane (20) and the ratio of secreted to intracellular infectivity is about 1:10 (21). Together, these observations suggest that within a natural host, MeV infection may be entirely cell associated, and free particle formation may not be needed. Our focus in this study was to understand how MeV infections are transferred from myeloid to epithelial cells.

To study this process, we relied exclusively on primary cells that were derived from either blood or lungs of human donors. We differentiated circulating monocytes into macrophages and DCs. Monocyte-derived macrophages (MDMs) and DCs recapitulate the functional phenotypes of macrophages *in vivo* for allergy, parasitic infections, and certain cancers (22). Here we report that DCs and MDMs are both permissive for MeV infection. We also demonstrate formally that transfer of MeV from immune to epithelial cells requires the epithelial receptor nectin-4 (6, 8, 10) and that cell-to-cell contact is necessary for efficient MeV transfer.

MATERIALS AND METHODS

Ethics statement. All studies involving human subjects received University of Iowa Institutional Review Board approval. All adult subjects provided informed, written consent. No children were part of this study.

Isolation of primary human monocyte-derived macrophages. To isolate peripheral blood mononuclear cells (PBMCs), whole blood was collected from healthy human donors and separated by Ficoll-Paque (Thermo Fisher) gradients. To differentiate cells into macrophages, isolated monocytes were maintained in 100-mm dishes in complete RPMI 1640 medium (RPMI 1640 medium supplemented with 10% fetal bovine serum [FBS], 2 mM L-glutamine, 100 U/ml of penicillin, and 100 U/ml of streptomycin) supplemented with either human granulocyte-macrophage colony-stimulating factor (GM-CSF; 50 ng/ml), human M-CSF (50 ng/ml), or human GM-CSF (50 ng/ml) plus human interleukin 4 (IL-4; 20 ng/ml). The culture medium was changed every 3 days. Macrophages were considered fully differentiated by 6 to 7 days of culture as defined by a change in morphology. After 6 to 7 days of differentiation, MDMs were activated toward particular phenotypes using different cytokine combinations. For the M1 phenotype, GM-CSF-induced MDMs were stimulated for 18 h with tumor necrosis factor alpha (TNF-α; 20 ng/ml) plus human gamma interferon (IFN-γ; 20 ng/ml). For the M2 phenotype, M-CSF-induced MDMs were activated for 18 h with human IL-4 (10 ng/ml) and human IL-13 (10 ng/ml). For DCs, monocytes were simply maintained for 6 to 7 days in human GM-CSF and human IL-4.

RT-qPCR. Total RNA from cells was purified using a Direct-zol RNA MiniPrep kit (Zymo Research, Irvine, CA) according to the manufacturer's instructions. The RNA concentration was determined with an ND-1000 spectrophotometer (NanoDrop). Total RNA (500 ng) was reverse transcribed by using a high-capacity reverse transcription (RT) kit (Thermo Fisher Scientific, Waltham, MA) according to the manufacturer's instructions. RT-quantitative PCRs (RT-qPCRs) were performed in an ABI Prism 7900 HT real-time PCR system (Thermo Fisher Scientific). The PCR conditions were as follows: 95°C for 10 min, 95°C for 15 s, and 60°C for 1 min for 40 cycles. The following primers were used in RT-qPCR analysis: for hCXCL9, CCACCCGAACGTCTTATCTAATC (forward) and GTGGGTCACAGACTCTCAAAT (reverse); for hCXCL10, TCTCC CATCACTTCCCTACAT (forward) and GGAGTAGTAGCAGCTGAT TTGG (reverse); for hCCL13, CAGAGGCTGAAGAGCTATGTG (forward) and CAGATCTCCTTGCCCAGTTT (reverse); and for hCCL17, GAGTACTTCAAGGGAGCCATTC (forward) and TGCCCTGCACAGT TACAAA (reverse). The results were analyzed using the software (SDS, version 2.3) provided by the instrument. The relative expression of the genes was calculated by the threshold cycle ($2^{-\Delta\Delta CT}$) formula using SFRS-9 as a normalizer. The values reported are means for at least three biological replicates, each with three technical replicates.

Cell culture. Primary cultures of human airway epithelia were prepared from trachea and bronchi by enzymatic dispersion using established methods (5). Briefly, epithelial cells were dissociated and seeded onto collagen-coated, semipermeable membranes with a 0.4-μm (number 3470; Corning, Lowell, MA) or 3-μm (number 3472; Corning) pore size (surface area, 0.33 cm^2). Human airway epithelial cultures were maintained in Ultroser G (USG) medium at 37°C and 5% CO_2. Polyester Transwell inserts were placed into 24-well plastic cell culture plates (Costar, Cambridge, MA). Twenty-four hours after seeding, the mucosal medium was removed and the cells were allowed to grow at the air-liquid interface as reported previously (5). Only well-differentiated cultures (>3 weeks old) were used in these studies. We note that the choice of insert was important because substantially reduced MeV infection was observed through alternative membrane materials (number 3413; Corning). The presence of tight junctions was confirmed by measuring the transepithelial resistance using a volt-ohm meter (World Precision Instruments, Sarasota, FL; resistance $> 500\ \Omega \cdot cm^2$).

MeV production and titer determination. MeV-GFP production was conducted as previously described (6, 23). MeV-GFP is a derivative of wild-type strain ICB-323 (24) expressing green fluorescent protein (GFP) from an additional transcription unit inserted upstream of the nucleocapsid gene (6). Briefly, Vero cells stably expressing the MeV receptor SLAMF1 (Vero-hSLAM cells) and cultured in Dulbecco's modified Eagle's medium (DMEM; Thermo Fisher Scientific, Waltham, MA) containing 8% newborn calf serum (NCS; Thermo Fisher Scientific) and penicillin-streptomycin (100 mg/ml; Thermo Fisher Scientific) were used to produce MeV-GFP. MeV-GFP titers of approximately 1×10^7 50% tissue culture infective doses ($TCID_{50}$)/ml were obtained. MeV release into culture medium from infected immune cells was also quantified by plaque formation assay on Vero/hSLAM cells as described previously (6).

MeV infection of human MDMs and HAE. For MeV infection of MDMs or DCs, cells were first plated in 12- or 6-well plates with 50,000 to 300,000 cells per well and incubated with MeV-GFP (produced in Vero-hSLAM cells) at a multiplicity of infection (MOI) of 1 for 4 h. Cells were then washed three times with phosphate-buffered saline (PBS) and allowed to culture for 2 days in complete RPMI 1640. MeV-infected MDMs or dendritic cells were dislodged using 0.25% trypsin–1 mM EDTA and cell scraping and resuspended in 50 μl of MEM. For basolateral infection of HAE, the Transwell culture insert containing the airway epithelial culture was turned over. Free virus or infected immune cells were applied for 4 h; then the inserts were washed with 1× PBS and returned to the upright position. For apical infection, free virus or infected immune cells were simply applied to the apical surface. Alternatively, Transwell culture inserts containing the airway epithelial cultures were scratched on the apical

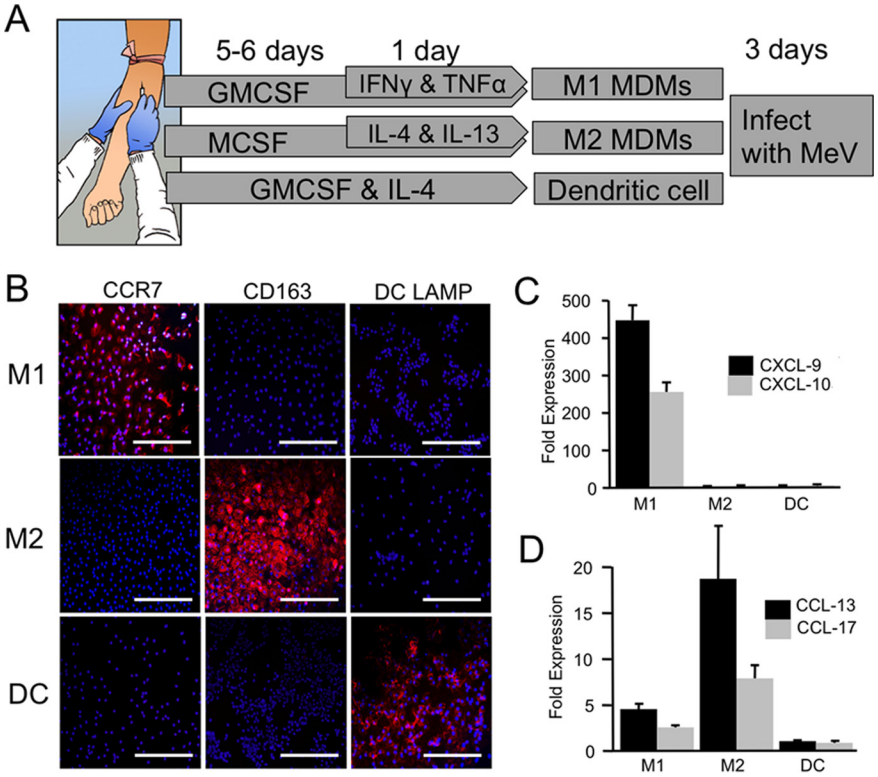

FIG 1 Characterization of human myeloid cells during differentiation. (A) Schematic of differentiation and polarization culture conditions for the human monocytes into M1 MDMs, M2 MDMs, and DCs. (B) DCs, M1-MDMs, and M2-MDMs were immunostained with DC-specific marker DC-LAMP, M1-specific marker CCR7, and M2-specific marker CD163. Scale bars = 100 μm. RNA was collected from DCs and MDMs at day 7. M1-specific (C) and M2-specific (D) biomarkers were analyzed using RT-qPCR assays. Data are expressed as mean fold change ± standard error ($n = 3$).

side with a 200-μl pipette tip to expose the basolateral surface, and free virus or infected immune cells were applied to the apical surface. As before, the suspension of MeV-infected cells or free virus was allowed to incubate with HAE for 4 h. After incubation, airway epithelial cultures were washed with 1× PBS. The cultures were then allowed to incubate at 37°C and 5% CO_2 for 3 days unless otherwise indicated.

SLAMF1 surface staining and fluorescence-activated cell sorter (FACS) analysis. For cell surface staining for SLAMF1 (CD150), 1×10^6 cells were first blocked with 1 μg of human IgG and incubated with 1 μg of anti-CD150 phycoerythrin (PE)-conjugated (number 12-1502; eBioscience, San Diego, CA) antibodies on ice. Cells were then fixed and permeabilized with Cytofix/Cytoperm solution (number 554722; BD Biosciences, San Jose, CA). All flow cytometry data were acquired on a BD FACSVerse (BD Biosciences) and were analyzed using FlowJo software (Tree Star Inc.).

Imaging and confocal microscopy. After the desired times postinfection, the cells were initially imaged on an inverted UV fluorescence microscope and then processed further for confocal microscopy. For processing, the cells were fixed in 2% paraformaldehyde, permeabilized in 0.2% Triton X-100, and blocked in 1% bovine serum albumin (BSA) for 1 h. For immunostaining, HAE were stained with primary antibodies anti-hCD14 (1:200; R&D Systems, Minneapolis, MN) overnight at 4°C, followed by 1 h of incubation with either Alexa Fluor 488-labeled goat anti-sheep, Alexa Fluor 568-labeled goat anti-sheep, or Alexa Fluor 568-labeled goat anti-rabbit secondary antibody (Life Technologies). The Transwell inserts containing the cells were separated from the plastic cylinder by cutting the edges with a razor blade and mounted on a slide with Vectashield with 4′,6-diamidino-2-phenylindole (DAPI; Vector Laboratories Inc., Burlingame, CA). The cells were visualized and photographed on a Leica TCS SP3 confocal microscope (Leica Microsystems Inc., Buffalo Grove, IL) using a 40× oil immersion objective. Three-dimensional (3D) reconstructions of the cells were built from ~80 to 90 optical z-stacks (step size of 1 μm) using ImageJ 1.47v software.

Nectin-4 monoclonal antibody (MAb) blocking assay. Scratched HAE were washed and incubated with 10 μg of anti-Nectin-4 clone N4.61 (EMD Millipore) or isotype controls at 37°C for 1 h. After antibody incubation, the suspension of MeV-infected cells or free virus was delivered to HAE for 4 h. Following the infection period, HAE were washed with 1× PBS. The cultures were then allowed to incubate at 37°C and 5% CO_2 for 3 days unless otherwise indicated.

Statistical analysis. Data are presented as means ± standard errors of individual data points. Statistical significance between groups was determined by Student's *t* test.

RESULTS

MeV infection of myeloid cells. Myeloid cells include leukocytes such as monocytes, macrophages, and dendritic cells (DCs). Nonhuman primate studies suggest that myeloid cells may deliver MeV to airway epithelial cells (14–17), but the mechanisms of virus transfer are poorly understood. To assess how permissive different types of myeloid cells are for MeV infection, we first collected primary monocytes from human blood donors and differentiated them into monocyte-derived macrophages (MDMs) or DCs. MDMs were generated using two different protocols (shown schematically in Fig. 1A). Protocol 1 yields a proinflammatory population of macrophages, termed M1 MDMs (25). Following differentiation, these cells express the appropriate markers, CCR7, CXCL-9, and CXCL-10 (Fig. 1B and C). MDMs

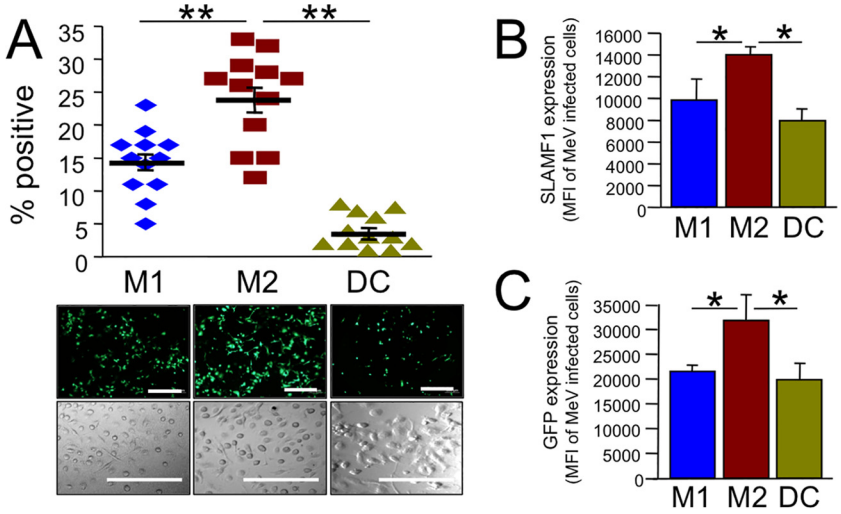

FIG 2 MeV infection of myeloid cells. (A) M1 MDMs, M2 MDMs, and DCs were infected with MeV-GFP at an MOI of 1. Two days postinfection, GFP expression was imaged by fluorescence microscopy (bottom images) and GFP-positive cells were quantified. Transmitted light images confirm similar confluence of cells. $n = 12$ donors. **, $P < 0.0001$. Scale bars = 100 μm. (B) Surface expression of MeV receptor SLAMF1 was determined by FACS analysis and is reported as the mean fluorescence intensity (MFI) in MeV-infected myeloid cell populations. Only SLAMF1$^+$ cells were included in the analysis. (C) The mean fluorescence intensity of GFP expression in MeV-infected myeloid cell populations was determined by FACS analysis. $n = 4$ donors. *, $P < 0.05$.

generated using protocol 2 express the markers CD163, CCL-13, and CCL-17 and represent an anti-inflammatory population (25) termed M2 MDMs (Fig. 1B and D). DCs were also generated using a standard protocol and express the marker DC LAMP (Fig. 1B). Following differentiation, the three populations of cells were infected with a wild-type strain of MeV expressing GFP (MeV-GFP) (6, 24). M2 MDMs were, on average, most permissive to MeV infection (Fig. 2A). To examine if expression of the MeV receptor (SLAMF1) correlates to infection, we measured the surface expression of SLAMF1 in the total cell population of M1 MDMs, M2 MDMs, and DCs. Within a population of myeloid cells, not all cells expressed SLAMF1, but >99% of all cells that expressed SLAMF1 were infected by MeV. SLAMF1 expression per MeV$^+$ cell was highest in M2 MDMs (Fig. 2B), suggesting that receptor density at the cell surface may contribute to MeV infection efficiency. In addition, the GFP intensity per MeV-infected cell was elevated in M2 MDMs (Fig. 2C). This may reflect increased MeV replication efficiency in this cell population.

M1 MDMs, M2 MDMs, and DCs deliver MeV to airway cells. We next asked which myeloid cells were best at delivering MeV to well-differentiated primary cultures of human airway epithelial cells (HAE). We previously showed that MeV preferentially infects HAE from the basolateral surface (4, 6–8). In our previous studies, MeV-GFP was delivered as "free" virus, i.e., virus that was purified from lysed producer cells and resuspended in serum-free medium. In this study, we first infected M1 MDMs, M2 MDMs, or DCs with free virus. Two days later, MeV-GFP-infected immune cells were applied to the apical (Fig. 3A) or basolateral (Fig. 3B)

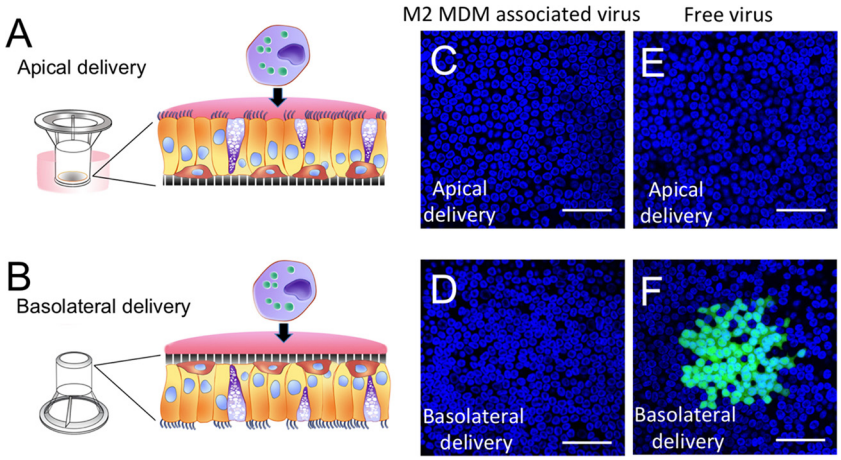

FIG 3 MeV-GFP-infected immune cells cannot transfer virus to intact HAE. Schematic apical (A) and basolateral (B) delivery protocols in HAE are shown. MeV-GFP-infected immune cells were delivered apically (C) or basolaterally (D) to the HAE for 4 h and then washed. Free MeV-GFP was delivered apically (E) or basolaterally (F) to the HAE for 4 h and then washed. Following the delivery period, the cultures were incubated at 37°C for 3 days, fixed, and counterstained with a nuclear DAPI stain (blue). Infectious centers (green) were formed only when free MeV was delivered basolaterally. HAE were grown on 0.4-μm-pore support membranes. Scale bars = 50 μm.

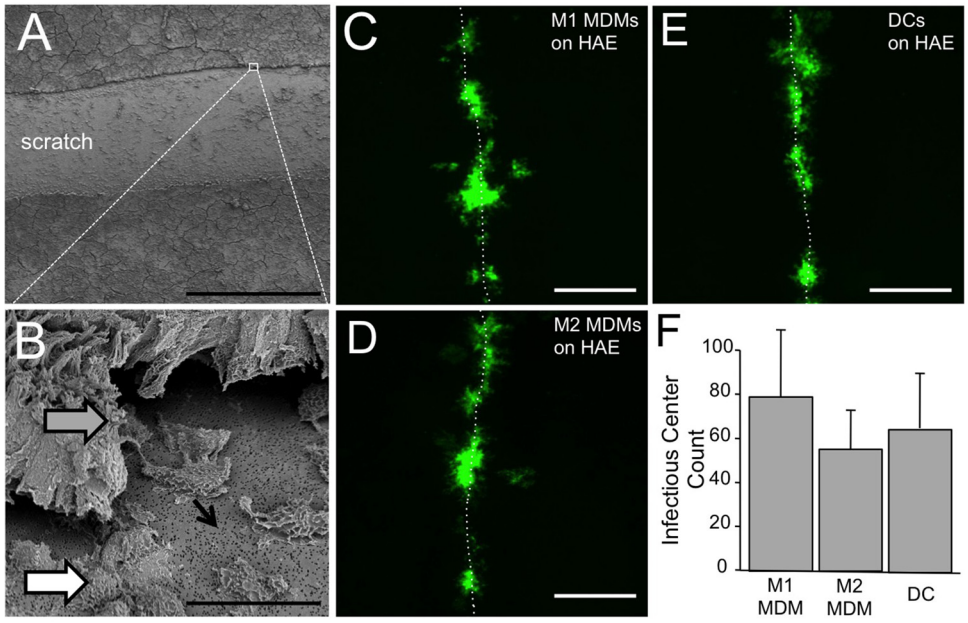

FIG 4 MeV-infected MDMs and DCs transfer MeV to scratched HAE. Scratched HAE were imaged using scanning electron microscopy at low power (A) and high power (B). Scale bars = 500 μm and 20 μm, respectively. Scratching temporarily exposes the lateral surfaces of columnar cells (gray arrow), basal cells (white arrow), and pores through the support filter (black arrow). Cell types in this model system have previously been characterized extensively based on morphological characteristics (5). Approximately 10^3 MeV-infected M1 MDMs (C), M2 MDMs (D), and DCs (E) were applied for 4 h. Scale bars = 500 μm. HAE cultures were then washed twice, and 3 days postinfection, GFP^+ infectious centers were imaged and counted. Infectious centers formed exclusively along the scratch, as indicated by dotted lines. (F) The number of infectious centers was determined by visual counting. $n = 6$.

surface of HAE cultures. We observed no transfer of MeV from immune cells to HAE using this protocol (Fig. 3C and D). In contrast, MeV free virus infection at the basolateral surface resulted in the expected infectious center formation (Fig. 3E and F). We hypothesized that access to the cellular receptor, nectin-4, was prevented either by tight junctions from the apical surface or by the support polyester membrane from the basolateral surface. Thus, this result was our first indication that cell-to-cell contact between infected myeloid cells and the basolateral surface of HAE may be necessary for MeV transfer.

Scratching polarized epithelia is a technique used by our laboratory and others to allow apically applied immune cells direct access to the basolateral cellular receptors (17, 26). The HAE are scratched by simply drawing a pipette tip across the cell surface with a gentle pressure sufficient to strip away cell layers not strongly adhered to the support membrane. Scanning electron microscopy of freshly scratched HAE demonstrated that the basolateral surface of columnar cells along the scratch is accessible (Fig. 4A and B). Approximately 10^3 MeV-GFP^+ M1 MDMs, M2 MDMs, or DCs were applied to the apical surface of scratched HAE. Three days later, HAE infectious centers were counted. For all lung donors, infectious centers were restricted to the immediate region of the scratch (Fig. 4C to E). No statistical difference was observed in the number of infectious centers conferred by M1 MDMs, M2 MDMs, or DCs (Fig. 4F). These data indicate that each of these cell populations can deliver MeV to airway epithelial cells. Scratching and wound repair have been described in detail for this HAE model (26); however, for these experiments, scratching was intended only to allow basolateral access for myeloid cells, not recapitulate a bona fide infection mechanism *in vivo*.

We previously reported that MeV spreads between columnar cells in HAE directly using points of cell-to-cell contact (7). In this study, we used confocal microscopy to monitor GFP expression transfer from infected MDMs to HAE. At 4 h after delivery of infected M2 MDMs to scratched HAE, GFP^+ MDMs were visible along the support membrane near the boundary of the scratch (Fig. 5A). At 24 h postdelivery, a z-stack of confocal images (Fig. 5B) and a 3D reconstruction (Fig. 5C) reveal a GFP^+ infectious center abutting a GFP^+ MDM. The yellow arrow indicates a faint green infectious center, the white arrow indicates a bright green MDM, and the red arrow indicates a point of contact (Fig. 5C). In addition, labeling for MeV N protein confirms that replicating virus was delivered and not just GFP (Fig. 5D and E). These data indicate that when MeV is delivered to HAE through infected MDMs, infectious centers are generated within 24 h. Equivalent results were obtained when M1 MDMs or DCs were used to deliver the viruses (data not shown).

Myeloid-cell-mediated MeV infection of HAE is nectin-4 dependent. Nectin-4 was identified as the epithelial receptor for MeV particle-based infections (6, 8, 10). To assess whether MeV transmission from myeloid cells to HAE requires nectin-4, we took advantage of a viral mutant with the capacity to use SLAMF1 as a cellular receptor but not nectin-4. This "nectin-4-blind" MeV infects immune cells with an efficiency equal to that of wild-type MeV but does not infect epithelial cells (6). We first infected M2 MDMs with wild-type MeV-GFP or nectin-4-blind MeV-GFP. Next, infected M2 MDMs were applied to the apical surface of scratched HAE. At 1 h postdelivery, individual GFP^+ M2 MDMs were visualized within the scratch of the epithelial sheet infected with either wild-type or nectin-4-blind virus (Fig. 6A and B). At 3 days postdelivery, infectious centers were observed in the cultures exposed to MDMs infected with wild-type MeV-GFP but not nec-

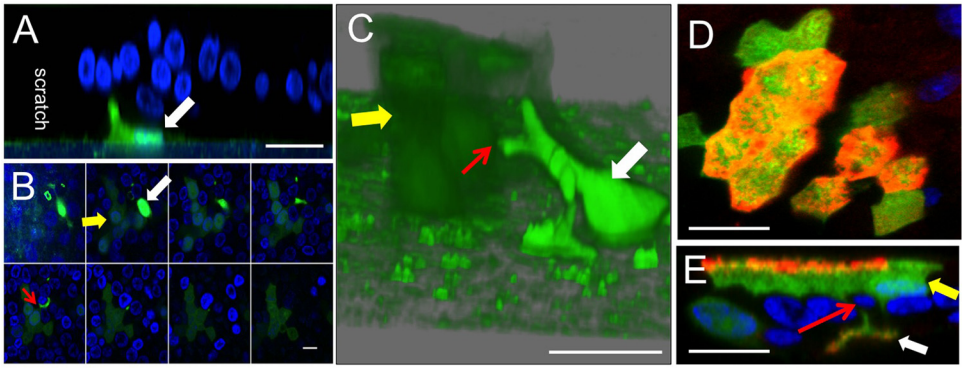

FIG 5 Cell-to-cell contact mediates delivery of MeV from MDMs to HAE. Human M2 MDMs were infected with MeV at an MOI of 1 for 4 h. After 48 h, MDMs were delivered to the apical surface of scratched HAE. After 4 h (A) or 24 h (B, C, D, and E), cultures were fixed and examined by confocal microscopy. (A) An MeV-GFP-infected MDM (white arrow) was observed at the edge of the scratch. (B and C) An infectious center (yellow arrow) formed near an MeV-GFP-infected MDM (white arrow). A cellular process from an infected MDM may contact an epithelial cell (red arrow). The three-dimensional reconstruction image in panel C was assembled from 38 optical z-stacks with a step size of 1 μm; in panel B every 4th z-stack is shown, from basolateral to apical. (D and E) MeV N protein colocalizes with GFP in MeV-infected immune cells and in an infectious center. At 24 h, cells were fixed, permeabilized with 0.2% Triton X-100, and incubated overnight with polyclonal antibodies against MeV N protein. N protein was visualized with a secondary antibody conjugated to Alexa Fluor 546 (red). An *xy en face* view (D) and an *xz* vertical view (E) are shown. Cell nuclei were visualized using DAPI (blue). Scale bars = 50 μm in panels A, C, D, and E and 20 μm in panel B.

tin-4-blind MeV-GFP (Fig. 6C and D). These data indicate that (i) by 3 days postdelivery, infected immune cells are undetectable and (ii) the transfer of MeV from immune cells to HAE is nectin-4 dependent. Equivalent results were obtained when M1 MDMs or DCs were used to deliver the viruses (data not shown). In a complementary experiment, scratched HAE were preincubated with a nectin-4 blocking antibody (Fig. 6E and F) or an isotype control antibody (Fig. 6G and H). No infection was subsequently observed with either free (Fig. 6E) or M2 MDM-delivered (Fig. 6F) MeV. Again, equivalent results were obtained when M1 MDMs or DCs were used to deliver the virus (data not shown).

Conditioned media from myeloid cells do not transfer infection to HAE. To further address the need for cell-to-cell contact to transmit MeV from infected immune cells to HAE, we collected conditioned media from infected immune cells. If MeV-infected M1 MDMs, M2 MDMs, or DCs simply allow for viral replication and release of free virus, then media collected from MeV-GFP-infected cells should contain enough viral particles to infect HAE. We observed that incubating scratched HAE with conditioned media did not result in the formation of infectious centers in any of the donors tested (Fig. 7A). However, when conditioned medium was applied to Vero-hSLAM cells, free virus was detected

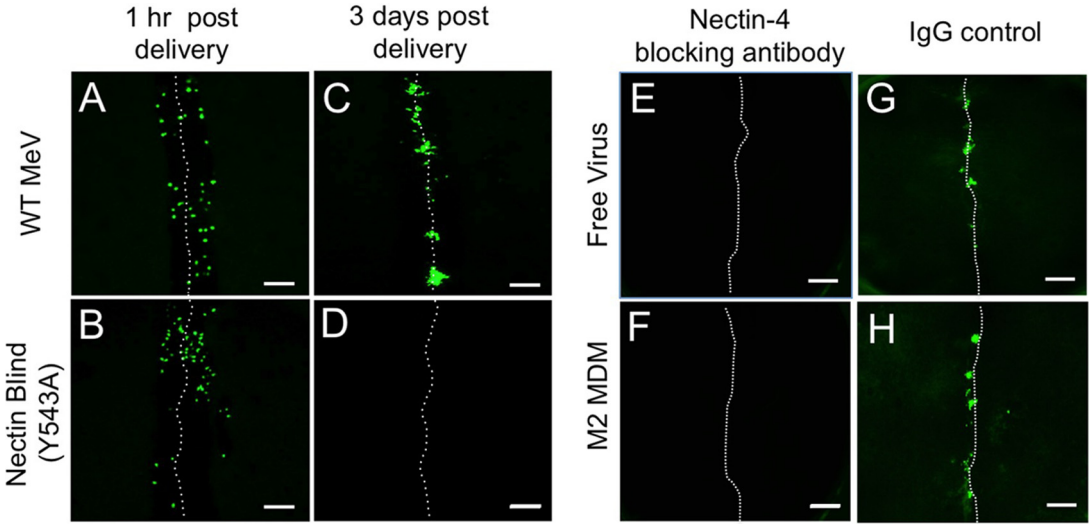

FIG 6 Cell-to-cell transmission of MeV-GFP from MDMs to HAE is nectin-4 dependent. M2 MDMs were infected with either MeV-GFP or nectin-blind MeV-GFP at an MOI of 1. Two days later, MDMs infected with wild-type MeV (A and C) or nectin-blind MeV (B and D) were applied to the apical surface of scratched HAE in 50 μl of medium. After 2 h, HAE were washed with PBS. The PBS was removed and the cells were then allowed to incubate at an air-liquid interface at 37°C and 5% CO_2 for 3 days. GFP expression was visualized by fluorescence microscopy at 1 h postdelivery (A and B) or 3 days postdelivery (C and D). Nectin-4 blocking antibody (E and F) or isotype control antibody (G and H) was preincubated with scratched HAE. Four hours later, free MeV (E and G) or MeV-infected M2 MDMs (F and H) were applied. Infectious centers were imaged 3 days later. The dotted line indicates the location of the scratch. Scale bar = 500 μm.

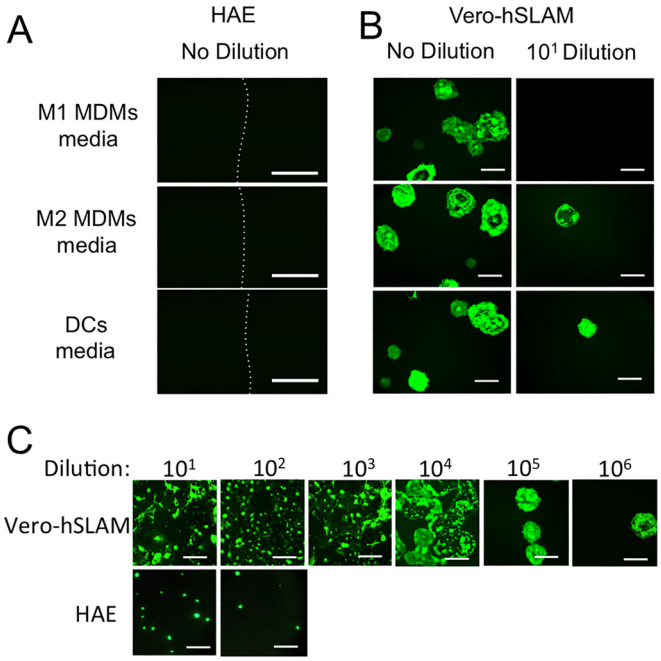

FIG 7 Conditioned media from myeloid cells do not transfer infection to HAE. Conditioned media collected from infected immune cells were applied to the apical surface of scratched HAE (A) or Vero-hSLAM cells (B) as indicated. GFP fluorescence was observed 3 days postinfection in Vero-hSLAM cells but not in HAE. (C) Dilutions of free MeV were applied either to Vero-hSLAM cells or to the basolateral surface of HAE for 4 h and then washed. Following a 3-day infection at 37°C, GFP fluorescence was imaged. HAE were grown on 0.4-μm-pore support membranes. Scale bars = 1 mm.

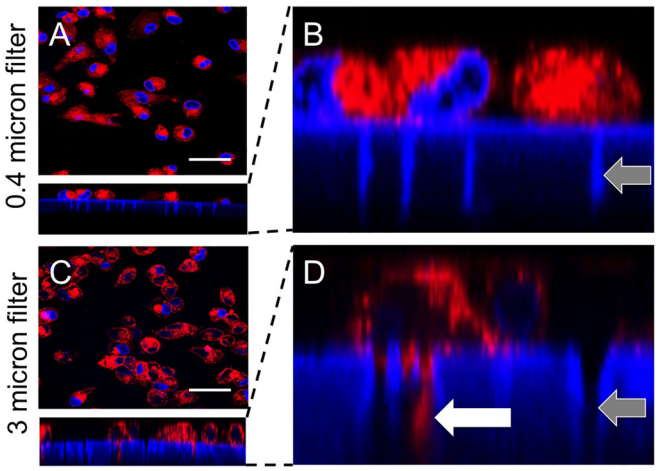

FIG 8 MDMs can penetrate large-pore but not small-pore support membranes. M2 MDMs were seeded onto small-pore (0.4-μm) (A and B) or large-pore (3.0-μm) (C and D) support membranes. Gray arrows indicate example pores. After 24 h, cell membranes were stained with CellMask (red). Nuclei were stained with DAPI (blue). Pseudopodial extensions were seen through the large-pore support membranes only (white arrow). Scale bars = 50 μm.

(Fig. 7B), albeit at extremely low titers (<10^2 PFU/ml for M1 MDMs, M2 MDMs, and DCs). This result was consistent with the observation that Vero-hSLAM cells are 1,000- to 10,000-fold more permissive to MeV infection than HAE (Fig. 7C). We conclude that levels of free virus released by M1 MDMs, M2 MDMs, or DCs are not sufficient for appreciable infection of HAE.

Contact-dependent transmission of MeV infection. Finally, we sought to assess whether infected myeloid cells applied to the basolateral side of Transwell inserts can transfer infection. CellMask (red) and DAPI (blue) were used to label M2 MDMs. DAPI also stains the exposed edges of the support membranes. When we seeded labeled M2 MDMs on HAE cultures grown in polyester Transwell inserts with a pore size of 0.4 μm, as in our previously published studies (4, 6–8), no pseudopods were detected penetrating the polyester support membrane (Fig. 8A and B). However, when M2 MDMs were seeded on membrane supports with 3.0-μm pores, pseudopodia were observed within the pores (Fig. 8C and D). We systematically observed 100 individual MDMs on both large- and small-pore support membranes. No pseudopods were observed extending through the 0.4-μm pore, whereas 46% of the MDMs extended pseudopods through the 3.0-μm support membranes. Thus, even in the absence of chemoattractants, M2 MDMs probe through 3.0-μm support membranes.

We then assessed whether infected M2 MDMs transmit MeV to HAE when cell-to-cell contact is permitted through large-pore (3.0-μm) support membranes. GFP$^+$ M2 MDMs transmitted infection when applied basolaterally to HAE grown on 3.0-μm supports (Fig. 9A) but not to HAE grown on 0.4-μm supports (Fig. 9B). Consistent with our previous observations, GFP$^+$ M2 MDMs transmitted infection when apically applied to scratched HAE, regardless of the pore size of the support membrane (Fig. 9C and D). Thus, while MeV released from MDMs would undoubtedly have the capacity to traverse 0.4-μm pores (27, 28), viral transfer was observed only when physical contact was made possible using 3.0-μm supports.

Finally, we documented physical contact between MeV-infected M2 MDMs and HAE infectious centers through a 3.0-μm filter. At 4 h after delivery of MeV-GFP$^+$ M2 MDMs to the basolateral surface of HAE, pseudopods were observed penetrating the pores (Fig. 9E, red arrows). At 24 h, a GFP$^+$ MDM was observed beneath ~78% of infectious centers. An example is shown in Fig. 9F. The experiment was repeated on HAE from 3 human donors, and no infectious centers were observed following MeV-GFP$^+$ M1 MDM, M2 MDM, or DC application to the basolateral surface of 0.4-μm filters (Fig. 9G). Together, these data generated in a primary cell culture model system strongly suggest that cell-to-cell contact between immune and epithelial cells facilitates transmission of MeV.

DISCUSSION

Our results indicate that MeV spreads from myeloid cells to airway epithelial cells using nectin-4 and cell-to-cell contacts. Infected M1 MDMs, M2 MDMs, or DCs were incapable of transferring virus from the intact apical surface of well-differentiated HAE or through the 0.4-μm support membrane. However, efficient MeV transfer was observed when cell-to-cell contact was facilitated either by scratching the epithelia or by growing the epithelial cells on 3.0-μm filters. In both cases, confocal microscopy revealed points of cell-to-cell contact between infected immune cells and epithelial infectious centers.

Many viruses spread directly from cell to cell in their natural hosts (29, 30), which has at least three advantages. The first is speed: either partially or fully assembled particles can spread at sites of cell-to-cell contact by exploiting proximity (30). The sec-

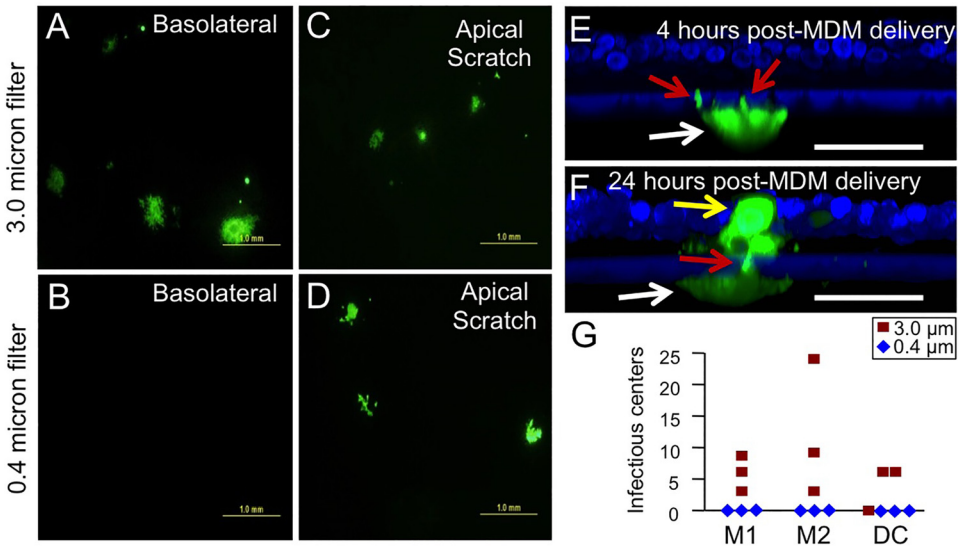

FIG 9 MDMs deliver virus through large-pore but not small-pore support membranes. MeV-infected M2 MDMs were applied to the basolateral surface of HAE grown on 3.0-μm-pore (A) or 0.4-μm-pore (B) support membranes. As controls, MeV-infected M2 MDMs were applied to the apical surface of scratched HAE grown on 3.0-μm-pore (C) or 0.4-μm-pore (D) support membranes. Scale bars = 1.0 mm. Three days postinfection, GFP^+ infectious centers were imaged. Cultures were fixed and examined by confocal microscopy (E and F). White arrows indicate an M2 MDM on the bottom surface of a support membrane, red arrows indicate macrophage filopodia traversing the support membrane, and the yellow arrow indicates an infectious center. Scale bars = 50 μm. (G) GFP^+ M1 MDMs, M2 MDMs, or DCs were delivered to the basolateral surface of 3.0-μm-pore or 0.4-μm-pore support membranes. The infectious centers were counted 3 days postdelivery. $n = 3$ human donors.

ond is immune evasion: limited exposure to the extracellular space can allow escape from neutralizing antibodies. The third is that epithelial barriers can be bypassed. Our analyses of MeV spread from immune to epithelial cells suggest that MeV remains cell associated not only during both the immune and the epithelial infection phases but also when infections are transferred between cell types.

Consistent with free MeV infection of HAE (7, 8), MeV spread from myeloid cells to HAE is nectin-4 dependent. Remarkably, several viruses use nectins or other proteins of the apical junction complex as receptors for entry in polarized epithelial cells (31) even if most of these proteins are not readily accessible. MeV and the other negative-strand RNA viruses of the genus *Morbillivirus* use nectin-4 (8–11, 32, 33), large DNA viruses like herpes simplex viruses 1 and 2 use nectin-1 and -2 (34–36), and the small positive-strand RNA virus poliovirus uses the poliovirus receptor PVR (37), also known as nectin-like protein 5. Moreover, other viruses use tight junction proteins, including occludins, claudins, and junctional adhesion molecules, as receptors (31). Exploiting adherens junction proteins is an effective way to overcome barriers within an organism in order to spread the infection.

A goal of this study was to identify the myeloid cells that productively deliver MeV to the basolateral surface of airway epithelial cells. We observed that all three cell types tested are permissive to MeV infection and can transfer it, but M2 MDMs are more permissive than M1 MDMs or DCs. This suggests that an anti-inflammatory population of macrophages may function as a primary vehicle for delivery. A recent study reported that MeV can spread from a human B-lymphoblastic (B-LCL) cell line to an immortalized human bronchial epithelium (HBE) cell line (17). Our results do not rule out the possibility that multiple myeloid-cell or lymphoid-cell-derived cell types are vehicles for MeV. Indeed, multiple cell types may contribute to systemic dissemination. Similarly, memory B cells have been shown to transfer Epstein-Barr virus to the basolateral surface of polarized epithelial cells (38).

In our study, infection levels of myeloid cells correlated with SLAMF1 protein surface expression. This may reflect increased infection efficiency or increased replication efficiency driven by the different proinflammatory and anti-inflammatory phenotypes of M1 MDMs and M2 MDMs, respectively (25, 39). The culture conditions that drive monocytes to differentiate and polarize into M1 MDMs include the cytokines IL-4 and IL-13, which may influence MeV replication. Furthermore, M1 MDMs produce proinflammatory cytokines (25, 40) and are inducible to produce antiviral factors, including interferon-regulating factors (41).

Our studies suggest that in natural hosts, infected myeloid cells deliver viral genomes directly to epithelial cells. Based on our results, we cannot discern if fully assembled viral particles that remain cell associated or only viral ribonucleocapsids are passed from cell to cell. We note that intercellular pores similar to those that form between columnar epithelial cells (7) would allow the transmission of many ribonucleocapsids. Transfer of large virus genome populations could enhance their fitness, promoting rapid readaptation to epithelia after extensive replication in immune cells. Future studies will assess whether this mechanism of virus transmission is based on the transfer of multiple genomes. Regardless, based on our *in vitro* model system, particle-independent, cell-based transmission appears to be an essential component of an evolutionary strategy that results in the extremely contagious nature of MeV.

Finally, in addition to creating new knowledge about MeV pathogenesis, our analyses may be relevant for cancer therapy. MeV is currently in clinical trials of oncolysis against five different cancer types (42, 43), and the gene for its receptor, nectin-4, is a

marker gene for lung, breast, and ovarian cancer (44–46). Consistently cell-associated MeV spread may favor oncolysis for the same reasons it favors viral spread: it is fast, it is shielded from neutralizing antibodies, and it bypasses epithelial barriers.

ACKNOWLEDGMENTS

We thank Rudragouda Channappanavar and Catherine Miller-Hunt for their technical help. We also thank Wendy Maury and Linda Powers for their monocyte differentiation consultations. Finally, we thank Mary Moye-Rowley for preparing the illustrations.

This work was supported by the National Institutes of Health grant R21 AI125747 (R.C. and P.L.S.). We acknowledge the support of the University of Iowa Genomics Division, In Vitro Models and Cell Culture Core, Viral Vector Core, and Cell Morphology Core.

REFERENCES

1. **Griffin DE.** 2013. Measles virus, p 1042–1069. *In* Knipe DM, Howley PM, Cohen JI, Griffin DE, Lamb RA, Martin MA, Roizman B (ed), Fields virology, 6th ed. Lippincott Williams and Wilkins, Philadelphia, PA.
2. **Blau DM, Compans RW.** 1997. Adaptation of measles virus to polarized epithelial cells: alterations in virus entry and release. Virology **231:**281–289. http://dx.doi.org/10.1006/viro.1997.8520.
3. **Blau DM, Compans RW.** 1995. Entry and release of measles virus are polarized in epithelial cells. Virology **210:**91–99. http://dx.doi.org/10.1006/viro.1995.1320.
4. **Sinn PL, Williams G, Vongpunsawad S, Cattaneo R, McCray PB, Jr.** 2002. Measles virus preferentially transduces the basolateral surface of well-differentiated human airway epithelia. J Virol **76:**2403–2409. http://dx.doi.org/10.1128/jvi.76.5.2403-2409.2002.
5. **Karp PH, Moniger TO, Weber SP, Nesselhauf TS, Launspach JL, Zabner J, Welsh MJ.** 2002. An in vitro model of differentiated human airway epithelia. Methods Mol Biol **188:**115–137.
6. **Leonard VH, Sinn PL, Hodge G, Miest T, Devaux P, Oezguen N, Braun W, McCray PB, Jr, McChesney MB, Cattaneo R.** 2008. Measles virus blind to its epithelial cell receptor remains virulent in rhesus monkeys but cannot cross the airway epithelium and is not shed. J Clin Invest **118:**2448–2458.
7. **Singh BK, Hornick AL, Krishnamurthy S, Locke AC, Mendoza CA, Mateo M, Miller-Hunt CL, Cattaneo R, Sinn PL.** 2015. The nectin-4/afadin protein complex and intercellular membrane pores contribute to rapid spread of measles virus in primary human airway epithelia. J Virol **89:**7089–7096. http://dx.doi.org/10.1128/JVI.00821-15.
8. **Mühlebach MD, Mateo M, Sinn PL, Prufer S, Uhlig KM, Leonard VH, Navaratnarajah CK, Frenzke M, Wong XX, Sawatsky B, Ramachandran S, McCray PB, Jr, Cichutek K, von Messling V, Lopez M, Cattaneo R.** 2011. Adherens junction protein nectin-4 is the epithelial receptor for measles virus. Nature **480:**530–533.
9. **Pratakpiriya W, Seki F, Otsuki N, Sakai K, Fukuhara H, Katamoto H, Hirai T, Maenaka K, Techangamsuwan S, Lan NT, Takeda M, Yamaguchi R.** 2012. Nectin4 is an epithelial cell receptor for canine distemper virus and involved in neurovirulence. J Virol **86:**10207–10210. http://dx.doi.org/10.1128/JVI.00824-12.
10. **Noyce RS, Bondre DG, Ha MN, Lin LT, Sisson G, Tsao MS, Richardson CD.** 2011. Tumor cell marker PVRL4 (nectin 4) is an epithelial cell receptor for measles virus. PLoS Pathog **7:**e1002240. http://dx.doi.org/10.1371/journal.ppat.1002240.
11. **Noyce RS, Delpeut S, Richardson CD.** 2013. Dog nectin-4 is an epithelial cell receptor for canine distemper virus that facilitates virus entry and syncytia formation. Virology **436:**210–220. http://dx.doi.org/10.1016/j.virol.2012.11.011.
12. **Tatsuo H, Ono N, Tanaka K, Yanagi Y.** 2000. SLAM (CDw150) is a cellular receptor for measles virus. Nature **406:**893–897. http://dx.doi.org/10.1038/35022579.
13. **Ferreira CS, Frenzke M, Leonard VH, Welstead GG, Richardson CD, Cattaneo R.** 2010. Measles virus infection of alveolar macrophages and dendritic cells precedes spread to lymphatic organs in transgenic mice expressing human signaling lymphocytic activation molecule (SLAM, CD150). J Virol **84:**3033–3042. http://dx.doi.org/10.1128/JVI.01559-09.
14. **Lemon K, de Vries RD, Mesman AW, McQuaid S, van Amerongen G, Yuksel S, Ludlow M, Rennick LJ, Kuiken T, Rima BK, Geijtenbeek TB, Osterhaus AD, Duprex WP, de Swart RL.** 2011. Early target cells of measles virus after aerosol infection of non-human primates. PLoS Pathog **7:**e1001263. http://dx.doi.org/10.1371/journal.ppat.1001263.
15. **Ludlow M, Rennick LJ, Sarlang S, Skibinski G, McQuaid S, Moore T, de Swart RL, Duprex WP.** 2010. Wild-type measles virus infection of primary epithelial cells occurs via the basolateral surface without syncytium formation or release of infectious virus. J Gen Virol **91:**971–979. http://dx.doi.org/10.1099/vir.0.016428-0.
16. **Frenzke M, Sawatsky B, Wong XX, Delpeut S, Mateo M, Cattaneo R, von Messling V.** 2013. Nectin-4-dependent measles virus spread to the cynomolgus monkey tracheal epithelium: role of infected immune cells infiltrating the lamina propria. J Virol **87:**2526–2534. http://dx.doi.org/10.1128/JVI.03037-12.
17. **Ludlow M, Lemon K, de Vries RD, McQuaid S, Millar EL, van Amerongen G, Yuksel S, Verburgh RJ, Osterhaus AD, de Swart RL, Duprex WP.** 2013. Measles virus infection of epithelial cells in the macaque upper respiratory tract is mediated by subepithelial immune cells. J Virol **87:**4033–4042. http://dx.doi.org/10.1128/JVI.03258-12.
18. **Monto AS.** 1999. Interrupting the transmission of respiratory tract infections: theory and practice. Clin Infect Dis **28:**200–204. http://dx.doi.org/10.1086/515113.
19. **McChesney MB, Miller CJ, Rota PA, Zhu YD, Antipa L, Lerche NW, Ahmed R, Bellini WJ.** 1997. Experimental measles. I. Pathogenesis in the normal and the immunized host. Virology **233:**74–84.
20. **Bohn W, Rutter G, Hohenberg H, Mannweiler K.** 1983. Inhibition of measles virus budding by phenothiazines. Virology **130:**44–55. http://dx.doi.org/10.1016/0042-6822(83)90116-2.
21. **Cathomen T, Naim HY, Cattaneo R.** 1998. Measles viruses with altered envelope protein cytoplasmic tails gain cell fusion competence. J Virol **72:**1224–1234.
22. **Sica A, Mantovani A.** 2012. Macrophage plasticity and polarization: in vivo veritas. J Clin Invest **122:**787–795. http://dx.doi.org/10.1172/JCI59643.
23. **Duprex WP, McQuaid S, Hangartner L, Billeter MA, Rima BK.** 1999. Observation of measles virus cell-to-cell spread in astrocytoma cells by using a green fluorescent protein-expressing recombinant virus. J Virol **73:**9568–9575.
24. **Takeda M, Takeuchi K, Miyajima N, Kobune F, Ami Y, Nagata N, Suzaki Y, Nagai Y, Tashiro M.** 2000. Recovery of pathogenic measles virus from cloned cDNA. J Virol **74:**6643–6647. http://dx.doi.org/10.1128/JVI.74.14.6643-6647.2000.
25. **Martinez FO, Gordon S, Locati M, Mantovani A.** 2006. Transcriptional profiling of the human monocyte-to-macrophage differentiation and polarization: new molecules and patterns of gene expression. J Immunol **177:**7303–7311. http://dx.doi.org/10.4049/jimmunol.177.10.7303.
26. **Vermeer PD, Einwalter LA, Moninger TO, Rokhlina T, Kern JA, Zabner J, Welsh MJ.** 2003. Segregation of receptor and ligand regulates activation of epithelial growth factor receptor. Nature **422:**322–326. http://dx.doi.org/10.1038/nature01440.
27. **Nakai T, Shand FL, Howatson AF.** 1969. Development of measles virus in vitro. Virology **38:**50–67. http://dx.doi.org/10.1016/0042-6822(69)90127-5.
28. **Rager M, Vongpunsawad S, Duprex WP, Cattaneo R.** 2002. Polyploid measles virus with hexameric genome length. EMBO J **21:**2364–2372. http://dx.doi.org/10.1093/emboj/21.10.2364.
29. **Mothes W, Sherer NM, Jin J, Zhong P.** 2010. Virus cell-to-cell transmission. J Virol **84:**8360–8368. http://dx.doi.org/10.1128/JVI.00443-10.
30. **Sattentau Q.** 2008. Avoiding the void: cell-to-cell spread of human viruses. Nat Rev Microbiol **6:**815–826. http://dx.doi.org/10.1038/nrmicro1972.
31. **Mateo M, Generous A, Sinn PL, Cattaneo R.** 2015. Connections matter—how viruses use cell-cell adhesion components. J Cell Sci **128:**431–439. http://dx.doi.org/10.1242/jcs.159400.
32. **Birch J, Juleff N, Heaton MP, Kalbfleisch T, Kijas J, Bailey D.** 2013. Characterization of ovine Nectin-4, a novel peste des petits ruminants virus receptor. J Virol **87:**4756–4761. http://dx.doi.org/10.1128/JVI.02792-12.
33. **Mateo M, Navaratnarajah CK, Willenbring RC, Maroun JW, Iankov I, Lopez M, Sinn PL, Cattaneo R.** 2014. Different roles of the three loops forming the adhesive interface of nectin-4 in measles virus binding and cell entry, nectin-4 homodimerization, and heterodimerization with nectin-1. J Virol **88:**14161–14171. http://dx.doi.org/10.1128/JVI.02379-14.
34. **Geraghty RJ, Krummenacher C, Cohen GH, Eisenberg RJ, Spear PG.** 1998. Entry of alphaherpesviruses mediated by poliovirus receptor-related

protein 1 and poliovirus receptor. Science **280:**1618–1620. http://dx.doi.org/10.1126/science.280.5369.1618.

35. **Eisenberg RJ, Atanasiu D, Cairns TM, Gallagher JR, Krummenacher C, Cohen GH.** 2012. Herpes virus fusion and entry: a story with many characters. Viruses **4:**800–832. http://dx.doi.org/10.3390/v4050800.
36. **Sakisaka T, Taniguchi T, Nakanishi H, Takahashi K, Miyahara M, Ikeda W, Yokoyama S, Peng YF, Yamanishi K, Takai Y.** 2001. Requirement of interaction of nectin-1alpha/HveC with afadin for efficient cell-cell spread of herpes simplex virus type 1. J Virol **75:**4734–4743. http://dx.doi.org/10.1128/JVI.75.10.4734-4743.2001.
37. **Mendelsohn CL, Wimmer E, Racaniello VR.** 1989. Cellular receptor for poliovirus: molecular cloning, nucleotide sequence, and expression of a new member of the immunoglobulin superfamily. Cell **56:**855–865. http://dx.doi.org/10.1016/0092-8674(89)90690-9.
38. **Shannon-Lowe C, Rowe M.** 2011. Epstein-Barr virus infection of polarized epithelial cells via the basolateral surface by memory B cell-mediated transfer infection. PLoS Pathog **7:**e1001338. http://dx.doi.org/10.1371/journal.ppat.1001338.
39. **Jaguin M, Houlbert N, Fardel O, Lecureur V.** 2013. Polarization profiles of human M-CSF-generated macrophages and comparison of M1-markers in classically activated macrophages from GM-CSF and M-CSF origin. Cell Immunol **281:**51–61. http://dx.doi.org/10.1016/j.cellimm.2013.01.010.
40. **Fleetwood AJ, Lawrence T, Hamilton JA, Cook AD.** 2007. Granulocyte-macrophage colony-stimulating factor (CSF) and macrophage CSF-dependent macrophage phenotypes display differences in cytokine profiles and transcription factor activities: implications for CSF blockade in inflammation. J Immunol **178:**5245–5252. http://dx.doi.org/10.4049/jimmunol.178.8.5245.
41. **Lacey DC, Achuthan A, Fleetwood AJ, Dinh H, Roiniotis J, Scholz GM, Chang MW, Beckman SK, Cook AD, Hamilton JA.** 2012. Defining GM-CSF- and macrophage-CSF-dependent macrophage responses by in vitro models. J Immunol **188:**5752–5765. http://dx.doi.org/10.4049/jimmunol.1103426.
42. **Miest TS, Cattaneo R.** 2014. New viruses for cancer therapy: meeting clinical needs. Nat Rev Microbiol **12:**23–34.
43. **Galanis E, Atherton PJ, Maurer MJ, Knutson KL, Dowdy SC, Cliby WA, Haluska P, Jr, Long HJ, Oberg A, Aderca I, Block MS, Bakkum-Gamez J, Federspiel MJ, Russell SJ, Kalli KR, Keeney G, Peng KW, Hartmann LC.** 2015. Oncolytic measles virus expressing the sodium iodide symporter to treat drug-resistant ovarian cancer. Cancer Res **75:**22–30. http://dx.doi.org/10.1158/0008-5472.CAN-14-2533.
44. **Derycke MS, Pambuccian SE, Gilks CB, Kalloger SE, Ghidouche A, Lopez M, Bliss RL, Geller MA, Argenta PA, Harrington KM, Skubitz AP.** 2010. Nectin 4 overexpression in ovarian cancer tissues and serum: potential role as a serum biomarker. Am J Clin Pathol **134:**835–845. http://dx.doi.org/10.1309/AJCPGXK0FR4MHIHB.
45. **Fabre-Lafay S, Garrido-Urbani S, Reymond N, Goncalves A, Dubreuil P, Lopez M.** 2005. Nectin-4, a new serological breast cancer marker, is a substrate for tumor necrosis factor-alpha-converting enzyme (TACE)/ADAM-17. J Biol Chem **280:**19543–19550. http://dx.doi.org/10.1074/jbc.M410943200.
46. **Takano A, Ishikawa N, Nishino R, Masuda K, Yasui W, Inai K, Nishimura H, Ito H, Nakayama H, Miyagi Y, Tsuchiya E, Kohno N, Nakamura Y, Daigo Y.** 2009. Identification of nectin-4 oncoprotein as a diagnostic and therapeutic target for lung cancer. Cancer Res **69:**6694–6703. http://dx.doi.org/10.1158/0008-5472.CAN-09-0016.